Macroscopic Quantum Coherence and Localization for Normal-State Electrons in Mg

N. B. Sandesara[a] and R. W. Stark
Department of Physics and Arizona Research Laboratories, University of Arizona, Tucson, Arizona 85721
(Received 2 August 1984)

Experiments utilizing electron quantum interferences manifested in the magnetoresistance of pure strain-free single crystals of magnesium have produced a new regime of magnetotransport characterized by quantum mechanical rather than semiclassical properties.

PACS numbers: 72.15.Gd, 72.15.Eb

One of the more intractable problems of solid state physics has been the achievement of long-range (~ 1 mm) coherence for the electron quantum states in a normal metal. In principle, such coherence should exist for a defect-free metal single crystal at 1 K where the density of weakly interacting quasiparticles (electrons, phonons, etc.) is low. For such a metal, many of the predicted experimentally measurable manifestations of long-range coherence result from the effects of an applied magnetic field, $\vec{H}$.

In the presence of $\vec{H}$, the one-electron Schrödinger equation can be expressed as

$$\left[\frac{1}{2m}\left(-ih\nabla-\frac{e}{c}\vec{A}\right)^2+V(\vec{r})\right]\psi_i(\vec{r})=E_i\psi_i(\vec{r}), \quad (1)$$

where $\vec{A}$ is the vector potential and $V(\vec{r})$ is the translationally invariant potential of the lattice of ion cores. Although Eq. (1) does not have a general solution, the semiclassical approximation is usually invoked to analyze the combined effects of $\vec{A}$ and $V(\vec{r})$.

By setting $\vec{A}=0$, Bloch's theorem can be invoked and Eq. (1) solved to obtain the energy band structure, $E(\vec{k})$, where $\vec{k}$ is the wave vector or quantum number of the electron. The electron is then treated as a wave packet with group velocity, $\vec{v}_{\vec{k}}=h^{-1}\nabla_{\vec{k}}E(\vec{k})$, that responds to a Lorentz force, $h\dot{\vec{k}}=(e/c)\vec{v}_{\vec{k}}\times\vec{H}$, to trace out a semiclassical trajectory, t. Quantization on t due to $\vec{A}$ is obtained by use of the phase integral:

$$\phi_t=(e/hc)\int_t\vec{A}\cdot d\vec{l}. \quad (2)$$

This approach has been remarkably successful in accounting for the observed properties of normal metals. The Lorentz force represents the time evolution of $\vec{k}(t)$ as $\vec{H}$ induces *intraband* transitions. When the state $\vec{k}(t)$ is near a Brillouin-zone plane, such time evolution can interfere with Bragg reflection and lead to *interband* transitions called *magnetic breakdown* (MB).[1,2] When MB occurs, the lattice of ion cores acts as a partially reflecting mirror for the electron wave packet with resultant probability amplitudes for transmission, p, and reflection, iq. These are related by $p^2=1-q^2=\exp(-H_0/H)$, where H_0 characterizes the strength of interaction of the electron with the Fourier component of $V(\vec{r})$ responsible for the Bragg reflection. Thus, MB can create extended networks of coupled semiclassical electron trajectories upon which probability amplitude evolves via a multitude of mutually interfering paths.

Figure 1 shows sections of the path segments in $\vec{k}$ space that produce a network of coupled trajectories that extend indefinitely and repetitively when $\vec{H}$ is applied along a $[10\bar{1}0]$-type axis of a Mg single crystal. The electron's motion in $\vec{r}$ space is characterized by two constants of motion, $\vec{k}\cdot\hat{H}$ and energy, as well as by $[\vec{r}(t)-\vec{r}_0]\times\hat{H}=hc\vec{k}(t)/eH$, where $\vec{r}(t)$ and $\vec{k}(t)$ are the position vectors of the time-evolving wave packet in planes perpendicular to $\vec{H}$ in $\vec{r}$ space and $\vec{k}$ space, respectively, and $\vec{r}_0$ is

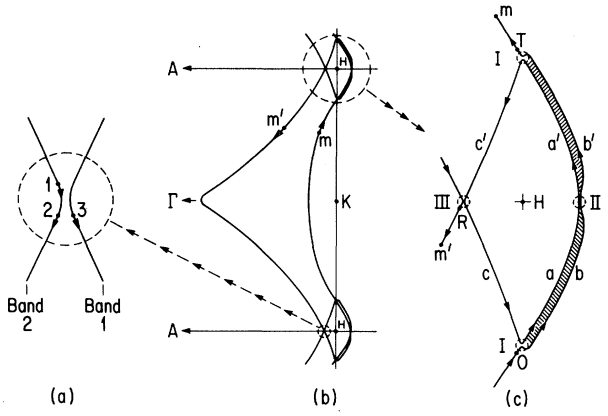

FIG. 1. (a) Schematic representation of interband tunneling caused by magnetic breakdown. Probability amplitude entering at 1 leaves at 2 and 3. (b) The ΓAHK Brillouin-zone–plane cross sections of the magnesium Fermi surface illustrating the electron trajectories that occur when $\vec{H}$ is applied along a $[10\bar{1}0]$-type axis. (c) Detail showing the "interferometer" trajectory segments that are coupled by magnetic breakdown at the points labeled I, II, and III.

an integration constant. One such trajectory, representable within a single Brillouin zone, exists in the $\vec{k}$-space plane shown in Fig. 1(b), but an ensemble exists of equivalent trajectories uniformly distributed in $\vec{r}$ space. Each of these, in containing continuous repetitions of the cell shown in Fig. 1(b), form an independent translationally invariant conducting chain.

The effects of the network shown in Fig. 1 upon the transverse magnetoresistance, $\rho(\vec{H})$, have been extensively investigated.[3,4] These studies utilized vapor-grown magnesium single crystals which were largely free of dislocations. Subsequent handling of these crystals to prepare experimental specimens invariably introduced lattice dislocations. The conclusions of these studies are summarized below.

(1) For $\vec{H}$ within 1° of $[10\bar{1}0]$, electron trajectories associated with the network shown in Fig. 1(b) totally dominate $\rho(\vec{H})$, which is characterized by τ_s, a small-angle–scattering lifetime for quantum dephasing. This differs from τ_l, the normal magnetotransport-momentum-relaxing lifetime that is due to large-angle scattering from localized lattice defects such as impurities. The crystals used for our experiments had residual resistivity ratios that were exceptionally high. Typical values, $\rho(0)_{300\,\mathrm{K}}/\rho(0)_{1\,\mathrm{K}} \approx 10^7$, indicate that these crystals were nearly free of point defects which contribute to τ_l. In contrast, τ_s arises mainly from dislocations, whose Fourier transforms can be highly localized. For all of our studies $\tau_s \ll \tau_l$.

(2) When the dislocation density is high enough so that $v_F\tau_s$ (v_F is the wave-packet Fermi velocity) is significantly shorter than the smallest trajectory segment in the network shown in Fig. 1(c), then the network transmits probability *intensity*. This defines a completely semiclassical regime for $\rho(\vec{H})$.[3]

(3) The longer the path a wave packet traverses across a crystal, the more likely it is to cross a dislocation and be dephased. Thus, τ_s can be defined only for specific path lengths and differs for each nonequivalent path. In all previously published work, dislocation densities were high enough to cause dephasing within distances smaller than the dimension of a single cell of the linear chain. However, the dimensions of the small segments of the network shown in Fig. 1(c) were usually smaller than the typical distance between dislocations. Thus, they could be logically separated from the trajectory segments m and m' in Fig. 1(b) and treated as a quantum mechanical switching junction for probability amplitude in a network that otherwise transmitted probability intensity. The net effect of this is an $\vec{H}$-dependent translation of the electron's center of mass that can be observed as small oscillatory components of $\rho(\vec{H})$ as H is varied. Since no phase coherence existed on a scale comparable to the dimension of the periodic cell, $\rho(\hat{H})$ could be accurately calculated from semiclassical theory.[3]

We can now prepare, reproducibly, experimental samples with much lower dislocation densities. For these, $\rho(\vec{H})$ arising from the network is qualitatively different from previously reported values. An example of this is shown in Fig. 2 where the orientation of $\hat{H}$ relative to $[10\bar{1}0]$ is varied. In curve *a*, the two most apparent features of the new data are the oscillations labeled $n = 0, 1, 2, 3$ and the sharp central minimum at $\theta = 0°$. This central minimum has a half-width that is less than 0.01° which is consistent with the predictions of Ref. 3. Note in Fig. 2 that $\rho(\vec{H})$ is shown in units of $\rho(0)_{300\,\mathrm{K}}$; the oscillations, which increase exponentially with H, are 10^7 times larger than $\rho(0)_{1\,\mathrm{K}}$.

For contrast, curve *b* of Fig. 2 corresponds to $\rho(\vec{H})$ for all previously published data. Although interference oscillations were observed in $\rho(H)$ for fixed $\hat{H}$ as H was varied, they were much smaller than $\rho(H)$, their phases were independent of θ, and curves such as *b* showed no oscillatory structure.

Quantum oscillations in observable macroscopic properties such as $\rho(\vec{H})$ result from regions of $\vec{k}$ space in which quantum phases are stationary with respect to summations over all contributing states. Usually less than 1% of the volume of $\vec{k}$ space contributes with stationary phase. As a result of symmetry breaking for $\theta \neq 0°$, the two lobes of the interferometer trajectories, shown crosshatched in

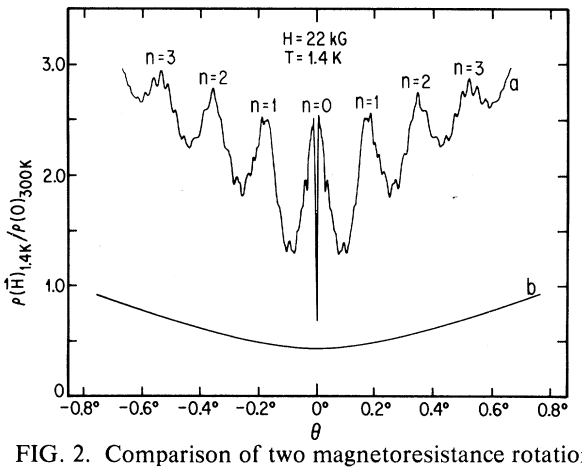

FIG. 2. Comparison of two magnetoresistance rotation diagrams showing the qualitative differences between the quantum regime (curve *a*) and the semiclassical regime (curve *b*). θ is the angle of deviation between $\hat{H}$ and $[10\bar{1}0]$ as $\hat{H}$ is rotated toward [0001].

Fig. 1(c), enclose different areas. By chance $\delta a(\theta)$, the difference between these two areas, though dependent on θ, is stationary over approximately 40% of the contributing states.[4] In units of area enclosing one flux quanta, for $H=22$ kG, at $\theta=0°$, $\delta a(\theta)=0$; at $\theta=\pm 0.2°$, $\delta a=1$, etc.; hence the labels $n=0,1,2,3$.

By arc discharge of a small capacitor at one end of the sample, we were able to introduce dislocations systematically. As the dislocation density increased, the first result was to eliminate the sharp $\theta=0°$ minimum and to eliminate the fine-structure oscillations in θ. Further increases caused both the amplitude of the large oscillations and the mean value of $\rho(\vec{H})$ to decrease. With additional arc discharge, curve *a* approached curve *b* and, just before becoming coincident with curve *b*, the $n=0,1,2,3$ oscillations changed phase by π. Surprisingly, this phase change agrees with the results of Ref. 4. There, $\rho(\vec{H})$ was calculated as a function of θ under the assumption $\tau_s=\infty$ for the switching junctions shown in Fig. 1(c) and with probability *intensity* transmission between junctions. It is apparent that the π phase shift corresponds to the onset of phase coherence *between* junctions.

Since the effect of dislocations is to produce momentum-conserving but phase-randomizing scattering relative to Eq. (2), an equivalent way to randomize phase is to introduce inhomogeneities into $\vec{A}$. Figure 3 shows the result of subjecting the sample to a small inhomogeneity, δH, superimposed upon $\vec{H}$. Curve *a* corresponds to a homogeneous field. Curves *b* and *c* correspond sequentially to increasing δH. The result is a reproducible and *reversible* mimic of the data produced *irreversibly* by increasing dislocation density.

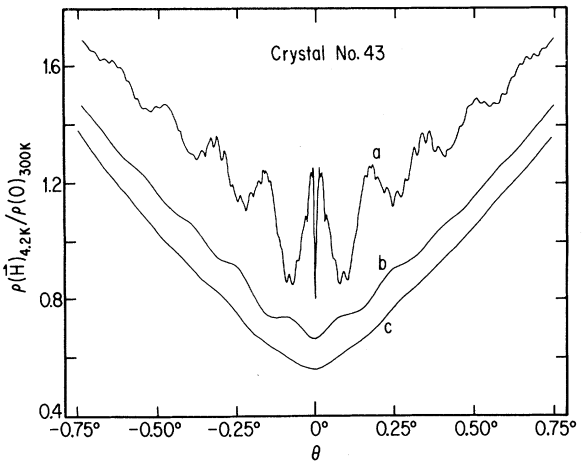

FIG. 3. The effects of increasing magnetic field inhomogeniety in the quantum regime for $H=20$ kG.

The amount of δH required to produce these effects was trivially small when compared with previous magnetoresistance standards. The phase difference $\Delta\phi_{mm'}=\phi_m-\phi_{m'}$ obtained by evaluating Eq. (2) for the paths in Fig. 1(b) for $H\approx 20$ kG, is $\Delta\phi_{mm'}\approx 10^4\pi$. The δH that produced curve *b* of Fig. 3 added a "randomizing" phase to $\Delta\phi_{mm'}$ of approximately π, i.e., it changed $\Delta\phi_{mm'}$ from cell to cell by about one part in 10^4. In this regime, $\rho(\hat{H})$ is so sensitive to δH that the current density, $\vec{j}$, used to measure $\rho(\hat{H})$ caused serious problems; $\vec{j}$ had to be kept below $\approx 10^{-3}$ A/mm^2 so that the magnetic field produced by $\vec{j}$ did not affect the measurement. We have concluded from our studies of the effects of δH and also from the linewidth of the central minimum that coherence extends over approximately twenty cells of the network for $H=22$ kG. This corresponds to a truly macroscopic quantum coherence distance that is greater than 0.1 mm.

It is apparent that a new regime of magnetotransport, dominated by quantum coherence, has been achieved for this normal metal. In contrast to normal $\rho(\vec{H})$ experiments, for this regime, $\rho(\vec{H})$ is manifestly sensitive to both small-angle scattering and weak inhomogeneities in $\vec{H}$. For $\theta\geq 0.005°$ and $H\approx 20$ kG, the magnitude of $\rho(\vec{H})$ is as much as an order of magnitude larger than equivalent semiclassical values; this clearly indicates that these new states tend to be localized. For larger values of H, the relative localization is much greater. These results are consistent with the predictions of Slutskin and Gorelik[5] for quantum-interference–generated electron localization on a "quasirandom" closed linear chain such as exists here for $\theta\neq 0°$.

We would like to thank Dr. C. B. Friedberg and Professor R. Reifenberger for their early contributions to this decade-long effort. This work was supported in part by National Science Foundation Grant No. DMR-8305282.

---

[a]Present address: Bell Communications Research, Holmdel, N.J. 07733.

[1]R. W. Stark and L. M. Falicov, in *Progress in Low Temperature Physics,* edited by C. J. Gorter (North-Holland, Amsterdam, 1967), Vol. 5.

[2]M. I. Kaganov and A. A. Slutskin, Phys. Rep. **98**, 189 (1983).

[3]R. W. Stark and R. Reifenberger, J. Low Temp. Phys. **26**, 763 (1977).

[4]D. Morrison and R. W. Stark, J. Low Temp. Phys. **45**, 531 (1981).

[5]A. A. Slutskin and L. Yu. Gorelik, Solid State Commun. **46**, 601 (1983).